Research on the adsorption property of supported ionic liquids for ferulic acid, caffeic acid and salicylic acid

Ni Du [a], Shuwen Cao [a,b], Yanying Yu [b,*]

[a] *State Key Laboratory of Food Science and Technology, Nanchang University, Nanchang 330047, Jiangxi, China*
[b] *Department of Chemistry, Nanchang University, Nanchang 330031, Jiangxi, China*

ABSTRACT

In this paper, the preparation of new supported ionic liquids (SILs) composed of the *N*-methylimidazolium cation and the quinoline cation is described. They have been confirmed and evaluated by infrared spectroscopy, elemental analysis and thermogravimetric analysis. Six kinds of different SILs included $SiO_2 \cdot Im^+ \cdot Cl^-$, $SiO_2 \cdot Im^+ \cdot BF_4^-$, $SiO_2 \cdot Im^+ \cdot PF_6^-$, $SiO_2 \cdot Qu^+ \cdot Cl^-$, $SiO_2 \cdot Qu^+ \cdot BF_4^-$ and $SiO_2 \cdot Qu^+ \cdot PF_6^-$. The adsorption characteristics of ferulic acid (FA), caffeic acid (CA) and salicylic acid (SA) on SILs were investigated by static adsorption experiments. It was found that $SiO_2 \cdot Qu^+ \cdot Cl^-$ had excellent adsorption and desorption capacity to three tested phenolic compounds. The dynamic adsorption characteristics of FA, CA and SA on $SiO_2 \cdot Qu^+ \cdot Cl^-$ were also studied. The saturated adsorption capacity of FA, CA and SA using $SiO_2 \cdot Qu^+ \cdot Cl^-$ as adsorbent was 64.6 mg/g, 53.2 mg/g and 72.2 mg/g respectively. Using 70% ethanol as eluent, the saturated desorption efficiencies of FA, CA and SA were 97.2%, 90.3% and 96.5% respectively. Thus, $SiO_2 \cdot Qu^+ \cdot Cl^-$ had strong adsorption and separation capacity for FA, CA and SA.

Crown Copyright © 2011 Published by Elsevier B.V. All rights reserved.

1. Introduction

Phenolic compounds are secondary plant metabolites and naturally present in almost all plant materials, including food products of plant origin. The ferulic acid (FA), caffeic acid (CA) and salicylic acid (SA) (Fig. 1) are phenolic compounds with prominent bioactivity and have been used widely in the medicine, food, and cosmetic industries. FA has many physiological functions, including anti-inflammatory, antithrombosis, anticancer activities, antioxidant, and immunomodulator [1,2]. CA and its derivatives are used as a component of antimitogen, anticancer activities, anti-inflammatory, antioxidant, antimelanin, and immunomodulator [3,4]. SA is required for signal transduction at the local level, and it can induce a wide variety of plants resistance to the virus, fungal and bacterial disease [5,6].

Recently, the conventional method for separation of phenolic compounds from the crude extracts was performed by solid–liquid extraction or solvent extraction, followed by polyamide column adsorption chromatography and gel chromatography [7]. But the separation technique involved in this method brought several problems including excessive solvent wastage, inefficiency in separation, solvents residual and operation insecurity. Besides, it was only fit for a small quantity of sample preparation, and not applicable for industrial practices.

Now, several methods have been used for pretreatment of the samples, such as solid-phase extraction. The key to solid-phase extraction was the selection of the solid-phase adsorbent, because it could control the analytical parameters such as selectivity, affinity and capacity [8,9]. Supported ionic liquids (SILs) which consist of bulky organic cations combined with inorganic or organic anions have recently been developed as a new adsorbent material. SILs have been successfully used in separation work due to its characteristic cations and anions [10,11]. However, there were relatively few reports on its application as a selective adsorbent in the separation and pre-concentration of certain activity components directly from natural plants. In this work, six kinds of different SILs were used as adsorbent to screen out the optimal separation and enrichment conditions of FA, CA and SA. Furthermore, the residue and the reuse of SILs were also discussed. It will extend the application of SILs in the separation and purification of plants.
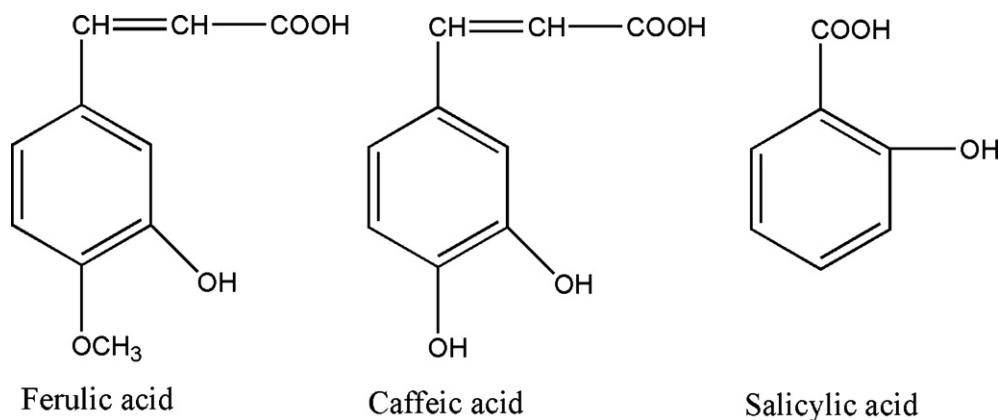
Fig. 1. Chemical structures of FA, CA and SA.

2. Experimental

2.1. Materials and reagents

All reagents and solvents were of analytical-reagent grade. Ethyl acetate, acetone, acetonitrile, N-methylimidazole (≥95%, Zhejiang Linhai Kaiyue Chemical Factory, China) and Quinoline (95%, Shanghai Tingxin Chemical Factory, China) were used with further dried and purification. Ammonium hexafluorophosphate (95%, Zhejiang Dongyang Dongcheng Chemical Factory, China), sodium tetrafluoroborate (Shanghai, China) and γ-chloropropyltrimethoxysilane (98%, Jingzhou Jianghan Fine ChemicalCo, Hubei, China) were used without further purification. Particles of Spherical macroporous silica gel (obtained from Qingdao YuMinYuan Silica gel reagent factory, Qingdao, China) had 40–70 μm mean particle sizes, and a surface area of 360 m^2/g. FA, CA and SA were obtained from Jiangsu Yancheng Langde Chem. Co. with nominal purity of more than 99%. Doubly distilled water was used for the experiment.

2.2. Preparation of SIL

1-Methylimidazole (or quinoline) and 3-chloropropyltrimethoxysilane (equal molar amount) was mixed at 100 °C for 24 h under argon atmosphere and then the residual reactants were washed three times with anhydrous ethyl acetate. Excess ethyl acetate was evaporated at 90 °C for 4 h. Im$^+$·Cl$^-$ or Qu$^+$·Cl$^-$ was then anion-exchanged by stirring it with NaBF$_4$ or NH$_4$PF$_6$ in acetone at room temperature for 3 days. Filtration and evaporation of the solvent afforded Im$^+$·BF$_4^-$, Im$^+$·PF$_6^-$ or Qu$^+$·BF$_4^-$, Qu$^+$·PF$_6^-$. Subsequently, water was removed from the silica gel using a Dean–Stark trap by refluxing in anhydrous toluene for 7 h. Then the Im$^+$·Cl$^-$, Im$^+$·BF$_4^-$, Im$^+$·PF$_6^-$ or Qu$^+$·Cl$^-$, Qu$^+$·BF$_4^-$, Qu$^+$·PF$_6^-$ were added to the acetonitrile/silica gel suspension and this mixture were refluxed for an additional 2 days.

Three kinds of SILs composed of the imidazolium cation had identified and approved by infrared spectroscopy, elemental analysis, and thermogravimetric analysis. The data were in good accordance with literature [12]. While, three kinds of new SILs composed of the quinoline cation were first synthesized in our laboratory with the pertinent literature as reference [12], the structures were characterized by infrared spectroscopy, elemental analysis, and thermogravimetric analysis. Chemical structures of SILs composed of the imidazolium cation and composed of the quinoline cation were listed in Fig. 2. Diffuse reflectance infrared Fourier transformation (DRIFT) spectra were obtained on an FTIR Nicolet5700 spectrometer (USA) in the range of 4000–400 cm^{-1}. The carbon, hydrogen and nitrogen contents of all the final materials were determined by elemental analysis that performed on a Vario

EL cube elemental analyzer (Elementar, Germany). Thermogravimetric curves were obtained on a PET series Thermal Analyzer from TG/DTA Pyris Diamond (USA) with a heating rate of 10 °C min^{-1} under nitrogen.

2.3. Static adsorption test

In the adsorption experiment, six kinds of SILs were tested as follows: same amount of SILs was put into an Erlenmeyer flask and the right amount of solution of FA, CA and SA was added. The flask was then shaken (100 rpm) in a water-bath shaker at a certain temperature. After that, solutions were collected and centrifuged at 3800 rpm for 10 min by a centrifuge, and then the absorbance of the supernatant was measured at 312 nm using UV-2450 spectrophotometer (Shimadzu, Japan) [13]. The adsorption efficiency was calculated by the following equations:

$$E(\%) = \frac{(c_0 - c_w) \times V}{c_0 \times V} \times 100$$
$$= \frac{c_0 - c_w}{c_0} \times 100$$

where C_0 and C_w represent the content of FA, CA and SA before and after pre-concentration (mg/mL), E (%) represents the adsorption efficiency percentage.
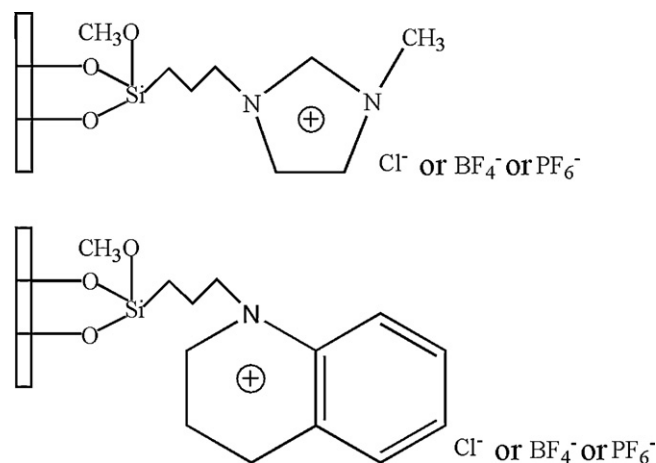

Fig. 2. Chemical structures of the supported ionic liquids composed of the imidazolium cation (a) and composed of the quinoline cation (b).

2.4. Dynamic adsorption test

For the column experiment, 10 g SILs was packed in a glass column (200 mm × 20 mm); certain concentration sample solution flowed through the glass column at a flow rate of 1.5 mL/min to test breakthrough point. When adsorption equilibration, the adsorbate-laden column was washed first with de-ionized water and then desorbed with ethanol–water (70:30, v/v) solution at the same flow rate, and its concentration was determined by spectrophotometry [13].

3. Results and discussion

3.1. Performance evaluation

FT-IR spectroscopy has been proven to be a powerful tool for providing conformational and structural information [14]. The spectra of quinoline SILs exhibited a characteristic absorption peak at the wavelength of 1530 cm^{-1}, 1527 cm^{-1} and 1567 cm^{-1} and the finger print region of C–N vibration was from 1500 to 1600 cm^{-1} [15]. This means that some C–N groups had interacted with the commercial silica.

The elemental contents of SiO$_2$·Qu$^+$·Cl$^-$, SiO$_2$·Qu$^+$·BF$_4^-$ and SiO$_2$·Qu$^+$·PF$_6^-$ were C 11.21%, N 1.13%, H 1.936%; C 8.94%, N 0.85%, H 1.27% and C 8.05%, N 0.78%, H 1.12%, respectively. From the percentage amounts of carbon, the bonding densities were 2.7 μmol/m^2, 2.2 μmol/m^2 and 2.0 μmol/m^2. The result showed that quinoline ionic liquids were bonded on the surface of silica successfully.

Based on the thermogravimetric analysis, there is an initial loss of weight at temperature below 100 °C for all samples. This is attributed to the removal of physically adsorbed water and/or any minor solvent residues remaining from the particle modification procedures [16]. This physically adsorbed water can be fully removed by further heating up to 100 °C [17]. The SILs composed of the quinoline cation shows two very distinct thermal events. For the first one, a pronounced increasing of 3.75%, 3.8% and 3.74% in mass loss was observed between 100 and 350 °C which is the organic moieties at the surface are expected to thermally decompose. On the other hand, a mass loss of 7.5%, 5.1% and 7.6% in the 350–800 °C range is associated with decomposition of the residual methoxy side groups.

3.2. The effect of adsorption conditions

The optimization process of different solvents, adsorption time, sample concentrations, solid–liquid ratio, and pH values were investigated. The saturated adsorption capacity of FA, CA and SA using SiO$_2$·Im$^+$·Cl$^-$, SiO$_2$·Im$^+$·BF$_4^-$, SiO$_2$·Im$^+$·PF$_6^-$, SiO$_2$·Qu$^+$·Cl$^-$, SiO$_2$·Qu$^+$·BF$_4^-$ and SiO$_2$·Qu$^+$·PF$_6^-$ as adsorbents were also investigated.

3.2.1. Effect of different solvents on the adsorption capacity

First of all, four batch tests with different polarities of organic solvents were conducted to elucidate the effect of solvents on the adsorption capacity and selectivity of the SILs. As shown in Fig. 3, the adsorption efficiencies were found to increase with the increase of the polarities of organic solvents. Adsorption efficiencies have reached a maximum in aqueous solution. So, aqueous solution is the optimum solvent by experiment.

3.2.2. Effect of adsorption time on the adsorption capacity

Experiments were conducted by Section 2.3. For the purpose of determining the optimum time of adsorption equilibrium, different time ranged from 10 to 120 min was investigated. Result showed that the adsorption efficiency of FA, CA and SA using SILs

Table 1
The effect of pH values on the adsorption ratio of FA.

SILs	pH values					
	1.64	2.71	3.67	4.69	5.53	6.58
SiO$_2$·Im$^+$·Cl$^-$	88.23	88.86	89.01	73.44	65.89	51.22
SiO$_2$·Im$^+$·BF$_4^-$	42.42	42.93	43.27	36.51	32.76	31.08
SiO$_2$·Im$^+$·PF$_6^-$	64.81	64.57	64.45	57.32	29.89	21.63
SiO$_2$·Qu$^+$·Cl$^-$	95.13	95.78	95.84	90.66	83.27	76.39
SiO$_2$·Qu$^+$·BF$_4^-$	77.13	77.32	76.97	70.93	63.84	53.18
SiO$_2$·Qu$^+$·PF$_6^-$	85.69	85.81	85.73	82.08	69.87	55.67

as adsorbent increased for 20 min reaching a plateau above 30 min. The distribution equilibrium of FA, CA or SA in two phases was arrived. Thus, in the following experiments, the adsorption time was set at 30 min.

3.2.3. Effect of solid–liquid ratio on the adsorption capacity

The adsorption process was conducted by the procedure described in Section 2.3. Different ratio of solid phase and liquid phase was investigated respectively. The initial concentration of the compounds was 1 mg/mL. From Fig. 4, we can see that with the solid–liquid ratio increasing to 2:50, the amount of eluted interferences was increased. When the solid–liquid ratio was more than 2:50, no more interference was observed. So, we select 2:50 as the optimum solid–liquid ratio.

3.2.4. Effect of sample concentration on the adsorption capacity

The adsorption efficiencies were calculated by changing the sample concentration. Results were obvious that the adsorption efficiency decreased with the increase of sample concentration because the high sample concentration reduced the distance of molecules. Therefore the interaction between sample molecules was enhanced, which would decrease the interaction between sample and SILs. Consequently, the adsorption efficiency decreased with the increase of sample concentration.

3.2.5. Effect of PH values on the adsorption capacity

The most important parameter influencing the adsorption capacity was the initial pH values of sample solution. It was related to the adsorption mechanisms onto the adsorbent surface from water and reflected the nature of the physicochemical interaction of FA, CA and SA in solution and the adsorptive sites of adsorbent. The pH values of FA, CA and SA of 500 mg/L were calculated at 3.42, 4.17, and 2.80 respectively. Since hydrochloric acid and sodium hydroxide were necessarily used to adjust pH. The adsorption efficiencies of FA, CA and SA at different values of pH were shown in Tables 1–3. The adsorption efficiencies increased greatly with the decrease of pH values.

The document [18] just released highlights research that SILs has strong capabilities of H-bonding, electrostatic repulsion, hydrophobic effect, anion exchange and dispersion force, etc. FA, CA and SA were mainly in the form of molecule in aqueous solution. The primary interaction forces between SILs and the compounds were mainly hydrogen bonding interaction between the nitrogen atoms

Table 2
The effect of pH values on the adsorption ratio of CA.

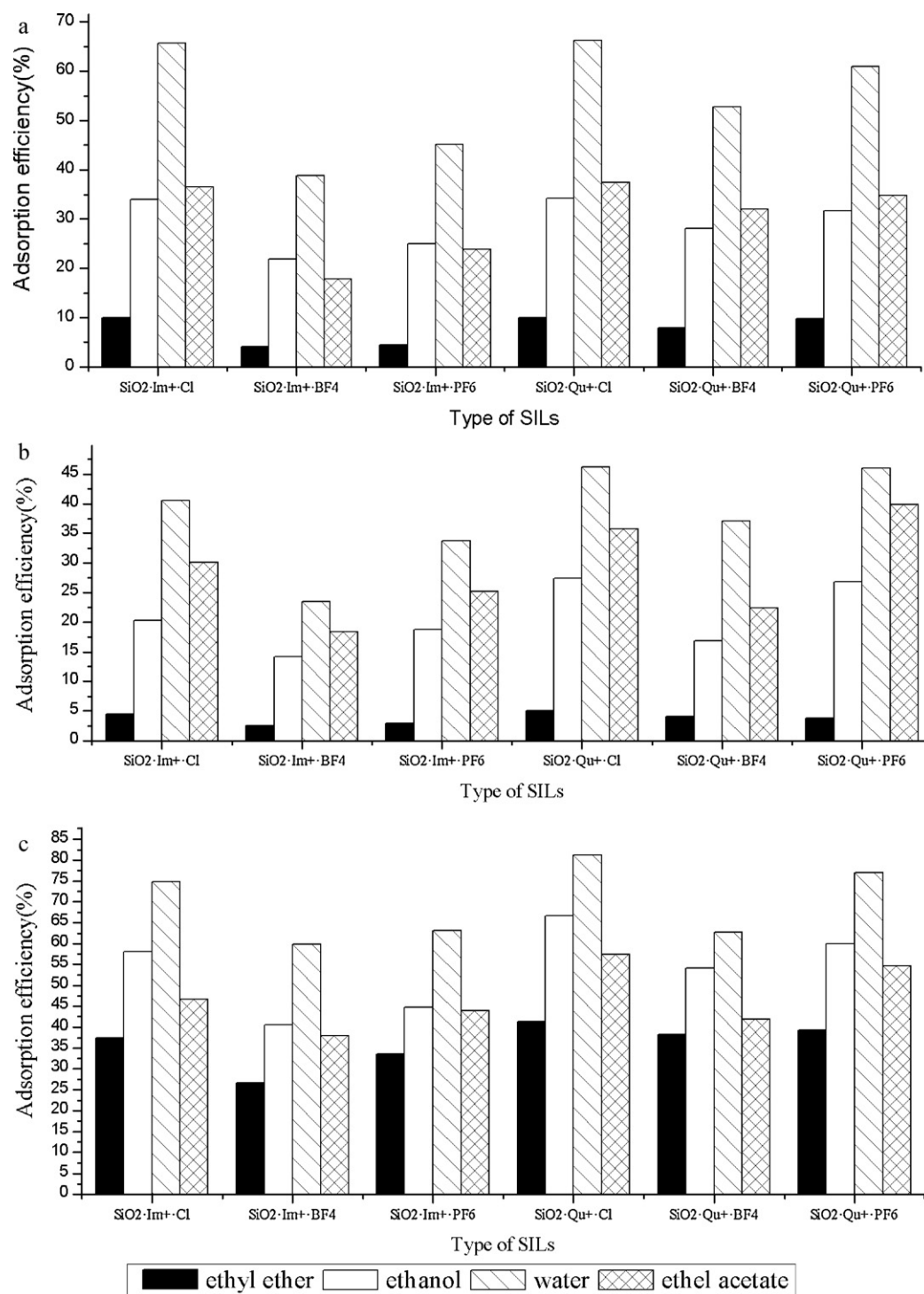| SILs	pH values					
	1.61	2.71	3.56	4.20	5.47	6.54
SiO$_2$·Im$^+$·Cl$^-$	81.97	81.73	81.85	81.66	65.92	50.43
SiO$_2$·Im$^+$·BF$_4^-$	26.98	27.15	27.33	27.41	14.82	10.88
SiO$_2$·Im$^+$·PF$_6^-$	56.36	55.19	55.27	54.29	31.67	22.75
SiO$_2$·Qu$^+$·Cl$^-$	90.81	90.34	90.29	89.93	73.85	66.27
SiO$_2$·Qu$^+$·BF$_4^-$	66.23	65.86	66.74	66.01	47.29	33.18
SiO$_2$·Qu$^+$·PF$_6^-$	83.82	82.95	83.73	82.96	69.12	58.07

Fig. 3. Variation charts of adsorption efficiency *vs.* solvent of FA (a), CA (b) and SA(c) using SIL as adsorbent.

Table 3
The effect of pH values on the adsorption ratio of SA.

| SILs	pH values								
	0.91	1.62	2.14	2.55	3.04	3.56	4.12	4.66	5.83
$SiO_2 \cdot Im^+ \cdot Cl^-$	96.18	96.13	96.28	96.13	96.09	90.04	84.18	76.72	70.25
$SiO_2 \cdot Im^+ \cdot BF_4^-$	71.24	71.45	71.32	71.45	71.57	65.43	60.63	53.85	46.96
$SiO_2 \cdot Im^+ \cdot PF_6^-$	84.26	84.42	83.99	84.13	84.16	79.24	71.69	64.83	58.91
$SiO_2 \cdot Qu^+ \cdot Cl^-$	98.86	98.98	99.07	99.16	99.15	95.67	90.32	83.37	77.82
$SiO_2 \cdot Qu^+ \cdot BF_4^-$	80.47	80.78	80.14	80.65	80.74	74.26	70.17	66.46	62.55
$SiO_2 \cdot Qu^+ \cdot PF_6^-$	93.83	93.59	93.26	93.18	93.15	88.78	83.36	78.75	73.29
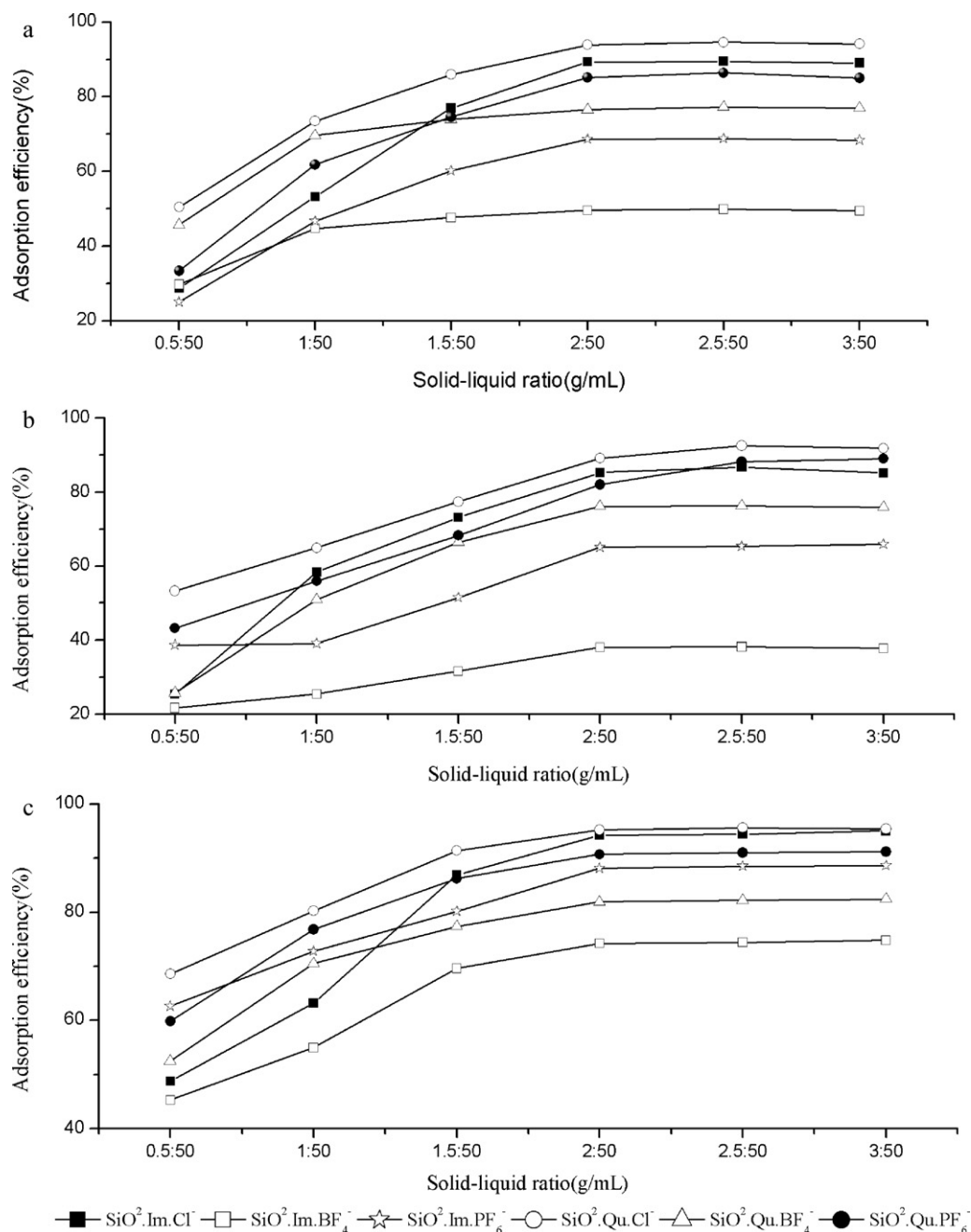
Fig. 4. Variation curves of adsorption efficiency *vs.* solid–liquid ratio of FA (a), CA (b) and SA(c) using SIL as adsorbent.

of the heteroatomic ring and the hydrogen atom from the hydroxyl of phenolic compounds and dispersion interaction between aromatic nucleus of phenolic compounds and heteroatomic ring of SILs in this experiment. The strength of these two interactions determined the adsorption efficiency. Then, the stronger these interactions were, the easier became the adsorption of FA, CA and SA from aqueous phase in SILs phase. The high adsorption efficiency of FA, CA and SA by SILs were then obtained.

The reasons indicated that with the increasing value of pH, the ionization of FA, CA and SA increased, which decreased the hydrogen bond interaction between FA (CA or SA) and SILs; the adsorption efficiency decreased. The hydroxyl ion in aqueous phase also increased with the increase of the pH value, and the electrostatic interaction between hydroxyl ion and cation of SILs decreased the electrostatic interaction between the carboxyl, phenolic hydroxyl anion of FA (CA or SA) and cation of SILs. Thus, the adsorption effi-

ciencies of FA, CA and SA by SILs decreased with the increase of pH value.

Summarizing our data on the adsorption of FA, CA and SA, we can conclude that the optimized conditions, which maximize the adsorptive capacity of phenolic compounds. It included the use of $SiO_2 \cdot Qu^+ \cdot Cl^-$ and a totally aqueous solution. The optimum time was 30 min, and 2:50 was the optimum solid–liquid ratio. The pH value should between 1.0 and 3.0 at least.

3.3. Dynamic adsorption and desorption of $SiO_2 \cdot Qu^+ \cdot Cl^-$

All the initial sample concentrations in this test were 1 mg/mL, the bed volume (BV) of $SiO_2 \cdot Qu^+ \cdot Cl^-$ was 19 mL, and the proper flow rate was 1.5 mL/min. When the dynamic adsorption reached equilibrium, the adsorbate-laden column was washed first by pure water, and then eluted with ethanol–water (70:30, v/v) solution at a
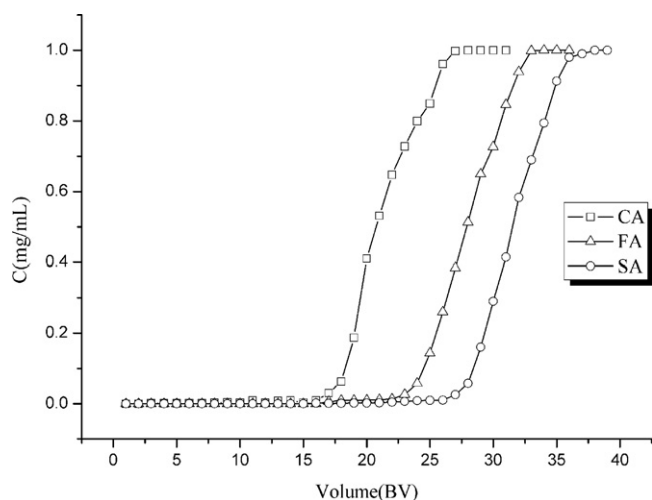
1702

N. Du et al. / J. Chromatogr. B 879 (2011) 1697–1703

Fig. 5. Dynamic adsorption curves of FA, CA and SA using $SiO_2 \cdot Qu^+ \cdot Cl^-$ as adsorbent.

Table 4
Adsorption ratio (E), desorption ratio (D) of different resins and $SiO_2 \cdot Qu^+ \cdot Cl^-$.

Sorbent	E (%)			D (%)		
	FA	CA	SA	FA	CA	SA
HPD-100	74.26	57.71	73.79	73.44	21.36	90.28
D101	80.15	63.86	84.23	75.54	16.85	58.51
AB-8	66.58	80.82	71.66	80.52	41.45	95.48
$SiO_2 \cdot Qu^+ \cdot Cl^-$	95.84	89.05	98.90	97.27	90.16	96.54

flow rate of 1.5 mL/min. As shown in Fig. 5, the processing volumes of three sample solutions were approximately 34, 28 and 38 BV. Therefore, the absorption capacities were 64.6 mg/g, 53.2 mg/g and 72.2 mg/g respectively.

In the dynamic desorption experiment, it was about that approximately 6 BV of ethanol–water (70:30, v/v) solution could elute the phenolic compound completely from $SiO_2 \cdot Qu^+ \cdot Cl^-$ at a flow rate of 1.5 mL/min. The saturated desorption efficiencies of FA, CA and SA were 97.2%, 90.3% and 96.5% respectively. Then desorption solution were dried under vacuum. The dried products were weighed and the contents of FA, CA and SA were calculated. The recovery yield of FA, CA and SA were 94.7%, 95.3% and 95.9%.

For the adsorption effect of the same phenolic compound using different SILs as adsorbent, it was very obviously that the intensity of dispersion interaction between the SILs composed of the quinoline cation was stronger than the SILs composed of the imidazolium cation, according to the number of aromatic ring. However, there were weak interfacial interaction between tetrafluoroborate or hexafluorophosphate-containing SILs and the compounds, due to the molecular weight and steric hindrance. Their adsorption capabilities were lower than chloride-containing SILs. Therefore, $SiO_2 \cdot Qu^+ \cdot Cl^-$ was the excellent one.

For the adsorption effect of different phenolic compounds using the same SILs as adsorbent, the intensity of hydrogen bonding and dispersion interaction were both different. According to the literature [19], hydrogen bonding could influence absorption peaks position and intensity, and usually made vibration frequency shift to lower wavenumber. That was for the rearrangement of the electronic distribution in the molecule by hydrogen bonding. It did not only decrease the force constant of the bond, but also brought down wavenumber. The stronger the hydrogen bonds formed, the more wavenumber decreased. For this reason, we researched the effects of hydrogen bonding through infrared spectroscopy. As shown in Fig. 6, we compared the characteristic absorption peak of C–N vibration in IR spectra before and after the adsorption of three phenolic compounds in two initial concentrations. It was shown that the previous peaks observed at $1530 \, cm^{-1}$ which originated from C–N vibration shift to lower wavenumber. In the two figures, the shift intensity of SA on $SiO_2 \cdot Qu^+ \cdot Cl^-$ was lower than FA or CA on $SiO_2 \cdot Qu^+ \cdot Cl^-$.

According to the literature [20], these wavenumber positions were influenced by hydrogen bonding interaction between the nitrogen atoms of the heteroatomic ring and the hydrogen atom from the hydroxyl of phenolic compounds. The chemical structures of FA and CA were similar. The difference was that the meta-

position and contraposition of FA were hydroxide and methoxyl group respectively. They could not form intramolecular hydrogen bond, which had slight influence on the hydrogen bonding interaction between FA and SILs. Because both the contraposition and metaposition of CA were hydroxide group, they easily formed intramolecular hydrogen bond, which reduced the hydrogen bonding interaction between CA and SILs. Thus, the adsorption efficiency of FA using the same SILs as adsorbent was higher than that of CA. While the orthoposition of SA were hydroxide group and carboxyl group, they easily formed intramolecular hydrogen bond, which reduced the hydrogen bonding interaction between SA and SILs. Above all, the intensity of hydrogen bonding interaction between FA and $SiO_2 \cdot Qu^+ \cdot Cl^-$ was higher than CA or SA.

However, the number of substitute groups on the benzene ring of SA was less than FA and CA. Comparatively, the intensity of dispersion interaction between SILs and SA was stronger than FA or CA due to its lower molecular weight and less steric hindrance. Therefore, SA was adsorbed in the largest amount of the three observed compounds.

It was known that the experiment results were consistent with theory analysis.

3.4. Contrast with macroporous resins

In recent years, macroporous resins have been increasingly viewed as an alternative for the separation and enrichment of effective components from many natural products [21,22]. In this study, $SiO_2 \cdot Qu^+ \cdot Cl^-$ and three macroporous resins with different properties were performed through adsorption and desorption experiments to test their adsorbent efficiency of the phenolic compounds. Based on relevant literature [23], the optimum conditions with macroporous resins were: the initial sample concentrations were 0.25 mg/mL, the flow rate was 1.5 mL/min, the contacting time was 6 h, the solid–liquid ratio was 1:6, and the pH value was 6.0. The optimum conditions with SILs were summarized on the above analysis. The results were listed in Table 4, $SiO_2 \cdot Qu^+ \cdot Cl^-$ had relatively higher adsorption ratio and desorption ratio, compared with the three resins. Therefore, $SiO_2 \cdot Qu^+ \cdot Cl^-$ was the good solid-phase adsorbent for FA, CA and SA.

3.5. Residual and reuse of SILs ($SiO_2 \cdot Qu^+ \cdot Cl^-$)

The residual in recovered solution is ionic liquids which were eluted from silica gel. It was obtained by detecting the content of element chlorine by turbidimetry [24]. The detection results suggested that residue of element chlorine was 13.1 ppm, so the residue of ionic liquids calculated was 92.8 mg/L.

The $SiO_2 \cdot Qu^+ \cdot Cl^-$ after elute using mixture solvent and methanol was washed by methanol over and over until the color of the modified silica showed pale yellow, then dried under vacuum at $50\,°C$ for 6 h. Sequentially, the SILs could be reused for further separation. The experiment results showed that $SiO_2 \cdot Im^+ \cdot Cl^-$ were used at least up to three times with unchanged the capacity of concentration separation, the total concentration rate could still reach 92.6%. After three uses, it would reduce the content of ionic liquids on the silica surface. Thus, the interaction force between SILs and phe-
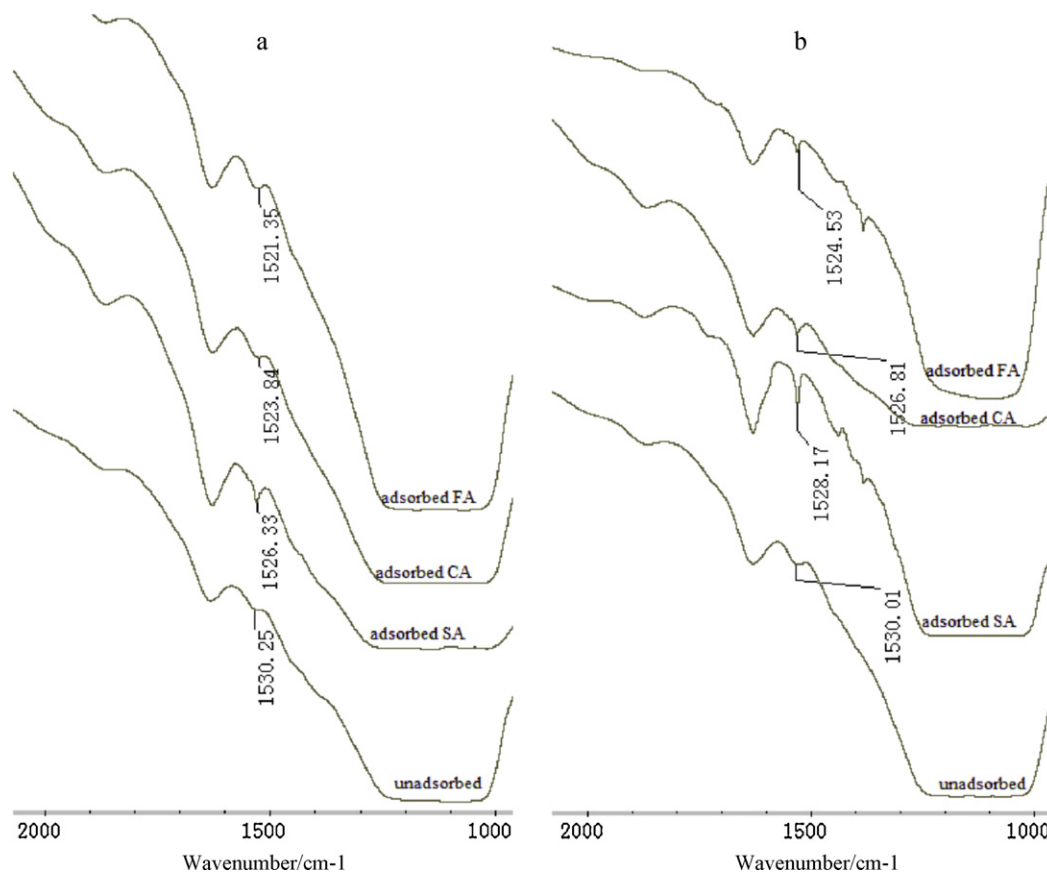
Fig. 6. Comparison IR spectrum (the characteristic absorption peak of C–N vibration) before and after the adsorption of three phenolic compounds. (The initial concentration was 0.1 mg/mL (a), 0.05 mg/mL (b) respectively.)

nolic compounds could be weaker, which lead to the decrease of adsorption effect.

4. Conclusions

The change between cation and anion's structure led to the difference of separation and enrichment capacity. In this study, the adsorption and desorption properties of six kinds of different SILs were evaluated and the separation process of FA, CA and SA using the selected SILs as adsorbent was optimized.

Result showed that the adsorption efficiency and the recovery of FA, CA and SA using $SiO_2 \cdot Qu^+ \cdot Cl^-$ as adsorbent were high. The effect of this new adsorbent was clearly superior to traditional adsorbent macroporous resins. Furthermore, the residual of SILs was low and it could be recycled three times. Therefore, it was worth further research that SILs was applied in separation and purification of active components from natural products.

Acknowledgements

References

[1] M. Srinivasan, A. Ram Sudheer, K. Raveendran Pillai, P.P. Raghu Kumar, R. Sudhakaran, V.P. Menon, Toxicology 228 (2006) 249.
[2] J. Kanski, M. Aksenova, A. Stoyanova, D.A. Butterfield, J. Nutr. Biochem. 13 (2002) 273.
[3] İlhami Gülçin, Toxicology 217 (2006) 213.
[4] Y. Feng, Y.W. Lu, P.H. Xu, Y. Long, W.M. Wu, W. Li, R. Wang, Biochim. Biophys. Acta 1780 (2008) 659.
[5] Q. Hayat, S. Hayat, M. Irfan, A. Ahmad, Environ. Exp. Bot. 68 (2010) 14.
[6] H.Y. Zhang, L.C.H. Ma, M. Turner, H.X. Xu, X.D. Zheng, Y. Dong, S. Jiang, Food Chem. 122 (2010) 577.
[7] Q. Wei, X.H. Ma, Chin. Tradit. Patent Med. 23 (2001) 135.
[8] Z. Li, X. Chang, X. Zou, X. Zhu, R. Nie, Z. Hu, R. Li, Anal. Chim. Acta 632 (2009) 272.
[9] Y.Q. Cai, G.B. Jiang, J.F. Liu, Q.X. Zhou, Anal. Chem. 75 (2003) 2517.
[10] Y. Liu, X. Sun, F. Luo, J. Chen, Anal. Chim. Acta 604 (2007) 107.
[11] M.L. Tian, H.Y. Yan, K.H. Row, J. Chromatogr. B 877 (2009) 738.
[12] M. Li, P.J. Pham, T. Wang, Ch.U. Pittman, T. Li, Sep. Purif. Technol. 66 (2009) 1.
[13] J. Fan, Ch.L. Wu, H.Zh. Xu, J.J. Wang, Ch.Y. Peng, Talanta 74 (2008) 1020.
[14] H. Gremlich, B. Yan, Infrared and Raman Spectroscopy of Biological Materials, Marcel Dekker, New York, 2000.
[15] H. Fabian, W. Mantele, Infrared Spectroscopy of Proteins Handbook of Vibrational Spectroscopy, vol. 5, John Wiley and Sons, Chichester, 2002.
[16] J.A.A. Sales, F.P. Faria, A.G.S. Prado, C. Airoldi, Polyhedron 23 (2004) 719.
[17] L.M.L.A. Auler, C.R. Silva, K.E. Collins, C.H. Collins, J. Chromatogr. A 1073 (2005) 147.
[18] X.T. Geng, P. Ren, G.P. Pi, R.F. Shi, Zh. Yuan, Ch.H. Wang, J. Chromatogr. A 1216 (2009) 8331.
[19] A. Milani, C. Castiglioni, E.D. Dedda, S. Radice, G. Canil, A.D. Meo, R. Picozzi, C. Tonelli, Polymer 51 (2010) 2597.
[20] H.D. Qiu, Y.Y. Hu, X. Liu, S.X. Jiang, Chin. J. Chromatogr. 25 (2007) 293.
[21] Y.J. Fu, Y.G. Zu, W. Liu, C.L. Hou, L.Y. Chen, S.M. Li, X.G. Shi, M.H. Tong, J. Chromatogr. A 1139 (2007) 206.
[22] B.Q. Fu, J. Liu, H. Li, L. Li, F.S.C. Lee, X.R. Wang, J. Chromatogr. A 1089 (2005) 18.
[23] W.L. Li, Y.Q. Fan, Y.B. Ji, Y.P. Wang, Chin. J. New Drugs 16 (2007) 9.
[24] P.F. Li, Q. Li, G.X. Gu, J. Sci. Technol. Food Ind. 29 (2008) 259.